US011579028B2

(12) United States Patent
Tsai et al.

(10) Patent No.: US 11,579,028 B2
(45) Date of Patent: Feb. 14, 2023

(54) **TEMPERATURE COEFFICIENT OF OFFSET COMPENSATION FOR FORCE SENSOR AND STRAIN GAUGE**

(71) Applicant: **NEXTINPUT, INC.**, Mountain View, CA (US)

(72) Inventors: **Julius Minglin Tsai**, San Jose, CA (US); **Dan Benjamin**, Atlanta, GA (US)

(73) Assignee: **Nextinput, Inc.**, Mountain View, CA (US)

(*) Notice: Subject to any disclaimer, the term of this patent is extended or adjusted under 35 U.S.C. 154(b) by 0 days.

(21) Appl. No.: **16/757,225**

(22) PCT Filed: **Oct. 17, 2018**

(86) PCT No.: **PCT/US2018/056245**
§ 371 (c)(1),
(2) Date: **Apr. 17, 2020**

(87) PCT Pub. No.: **WO2019/079420**
PCT Pub. Date: **Apr. 25, 2019**

(65) **Prior Publication Data**

US 2021/0190608 A1 Jun. 24, 2021

Related U.S. Application Data

(60) Provisional application No. 62/573,271, filed on Oct. 17, 2017.

(51) **Int. Cl.**
G01L 1/22 (2006.01)
G01L 1/16 (2006.01)
G01L 1/18 (2006.01)

(52) **U.S. Cl.**
CPC ***G01L 1/2281*** (2013.01); ***G01L 1/16*** (2013.01); ***G01L 1/18*** (2013.01)

(58) **Field of Classification Search**
CPC G01L 1/2281; G01L 1/16; G01L 1/18
(Continued)

(56) **References Cited**

U.S. PATENT DOCUMENTS

4,276,533 A 6/1981 Tominaga et al.
4,594,639 A 6/1986 Kuisma
(Continued)

FOREIGN PATENT DOCUMENTS

CN 101341459 A 1/2009
CN 101458134 A 6/2009
(Continued)

OTHER PUBLICATIONS

Virginia Semiconductors. The General Properties of Si, Ge, SiGe, SiO2 and Si3N4. Jun. 2002. [retrieved on Dec. 11, 2018]. Retrieved from the Internet: <URL:https://www.virginiasemi.com/pdf/generalpropertiesSi62002.pdf>. entire document.
(Continued)

Primary Examiner — Octavia Davis Hollington
(74) *Attorney, Agent, or Firm* — Withrow & Terranova, P.L.L.C.

(57) **ABSTRACT**

MEMS force sensors for providing temperature coefficient of offset (TCO) compensation are described herein. An example MEMS force sensor can include a TCO compensation layer to minimize the TCO of the force sensor. The bottom side of the force sensor can be electrically and mechanically mounted on a package substrate while the TCO compensation layer is disposed on the top side of the sensor. It is shown the TCO can be reduced to zero with the appropriate combination of Young's modulus, thickness, and/or thermal coefficient of expansion (TCE) of the TCO compensation layer.

19 Claims, 6 Drawing Sheets

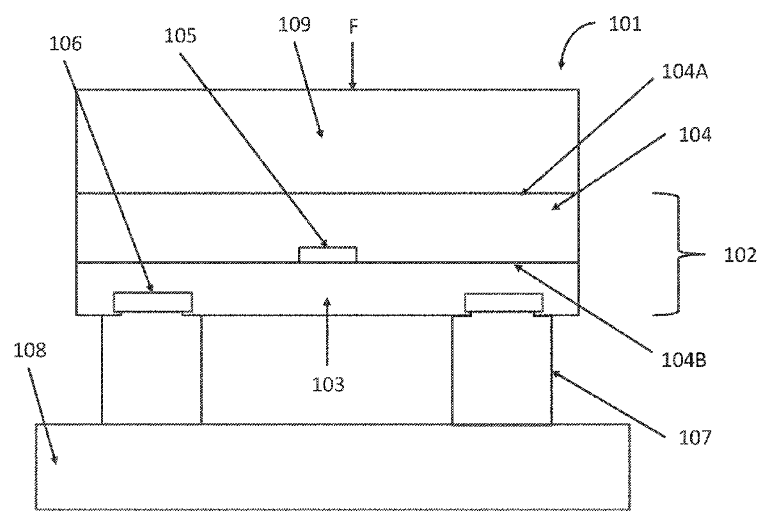

(58) **Field of Classification Search**
USPC 73/862.623
See application file for complete search history.

(56) **References Cited**

U.S. PATENT DOCUMENTS

4,658,651	A	4/1987	Le
4,814,856	A	3/1989	Kurtz et al.
4,842,685	A	6/1989	Adams
4,849,730	A	7/1989	Izumi et al.
4,914,624	A	4/1990	Dunthorn
4,918,262	A	4/1990	Flowers et al.
4,933,660	A	6/1990	Wynne
4,983,786	A	1/1991	Stevens
5,095,401	A	3/1992	Zavracky et al.
5,159,159	A	10/1992	Asher
5,166,612	A	11/1992	Murdock
5,237,879	A	8/1993	Speeter
5,291,795	A	3/1994	Hafner
5,320,705	A	6/1994	Fujii et al.
5,333,505	A	8/1994	Takahashi et al.
5,343,220	A	8/1994	Veasy et al.
5,349,746	A	9/1994	Gruenwald et al.
5,351,550	A	10/1994	Maurer
5,483,994	A	1/1996	Maurer
5,510,812	A	4/1996	O'Mara et al.
5,541,372	A	7/1996	Baller et al.
5,543,591	A	8/1996	Gillespie et al.
5,565,657	A	10/1996	Merz
5,600,074	A	2/1997	Marek et al.
5,661,245	A	8/1997	Svoboda et al.
5,673,066	A	9/1997	Toda et al.
5,679,882	A	10/1997	Gerlach et al.
5,760,313	A	6/1998	Guentner et al.
5,773,728	A	6/1998	Tsukada et al.
5,889,236	A	3/1999	Gillespie et al.
5,921,896	A	7/1999	Boland
5,969,591	A	10/1999	Fung
5,994,161	A	11/1999	Bitko et al.
6,012,336	A	1/2000	Eaton et al.
6,028,271	A	2/2000	Gillespie et al.
6,159,166	A	12/2000	Chesney et al.
6,243,075	B1	6/2001	Fishkin et al.
6,348,663	B1	2/2002	Schoos et al.
6,351,205	B1	2/2002	Armstrong
6,360,598	B1	3/2002	Calame et al.
6,437,682	B1	8/2002	Vance
6,555,235	B1	4/2003	Aufderheide et al.
6,556,189	B1	4/2003	Takahata et al.
6,569,108	B2	5/2003	Sarvazyan et al.
6,610,936	B2	8/2003	Gillespie et al.
6,620,115	B2	9/2003	Sarvazyan et al.
6,629,343	B1	10/2003	Chesney et al.
6,668,230	B2	12/2003	Mansky et al.
6,720,712	B2	4/2004	Scott et al.
6,788,297	B2	9/2004	Itoh et al.
6,801,191	B2	10/2004	Mukai et al.
6,809,280	B2	10/2004	Divigalpitiya et al.
6,812,621	B2	11/2004	Scott
6,822,640	B2	11/2004	Derocher
6,868,731	B1	3/2005	Gatesman
6,879,318	B1	4/2005	Chan et al.
6,888,537	B2	5/2005	Benson et al.
6,915,702	B2	7/2005	Omura et al.
6,931,938	B2	8/2005	Knirck et al.
6,946,742	B2	9/2005	Karpman
6,995,752	B2	2/2006	Lu
7,138,984	B1	11/2006	Miles
7,173,607	B2	2/2007	Matsumoto et al.
7,190,350	B2	3/2007	Roberts
7,215,329	B2	5/2007	Yoshikawa et al.
7,218,313	B2	5/2007	Marcus et al.
7,224,257	B2	5/2007	Morikawa
7,245,293	B2	7/2007	Hoshino et al.
7,273,979	B2	9/2007	Christensen
7,280,097	B2	10/2007	Chen et al.
7,318,349	B2	1/2008	Vaganov et al.
7,324,094	B2	1/2008	Moilanen et al.
7,324,095	B2	1/2008	Sharma
7,336,260	B2	2/2008	Martin et al.
7,337,085	B2	2/2008	Soss
7,343,233	B2	3/2008	Min et al.
7,345,680	B2	3/2008	David
7,367,232	B2	5/2008	Vaganov
7,406,661	B2	7/2008	Väänänen et al.
7,425,749	B2	9/2008	Hartzell et al.
7,426,873	B1	9/2008	Kholwadwala et al.
7,449,758	B2	11/2008	Axelrod et al.
7,460,109	B2	12/2008	Satai et al.
7,476,952	B2	1/2009	Vaganov et al.
7,508,040	B2	3/2009	Nikkei et al.
7,554,167	B2	6/2009	Vaganov
7,571,647	B2	8/2009	Takemasa et al.
7,607,111	B2	10/2009	Vaananen et al.
7,620,521	B2	11/2009	Breed et al.
7,629,969	B2	12/2009	Kent
7,637,174	B2	12/2009	Hirabayashi
7,649,522	B2	1/2010	Chen et al.
7,663,612	B2	2/2010	Bladt
7,685,538	B2	3/2010	Fleck et al.
7,698,084	B2	4/2010	Soss
7,701,445	B2	4/2010	Inokawa et al.
7,746,327	B2	6/2010	Miyakoshi
7,772,657	B2	8/2010	Vaganov
7,791,151	B2	9/2010	Vaganov et al.
7,819,998	B2	10/2010	David
7,825,911	B2	11/2010	Sano et al.
7,829,960	B2	11/2010	Takizawa
7,832,284	B2	11/2010	Hayakawa et al.
7,880,247	B2	2/2011	Vaganov et al.
7,903,090	B2	3/2011	Soss et al.
7,921,725	B2	4/2011	Silverbrook et al.
7,938,028	B2	5/2011	Hirabayashi et al.
7,952,566	B2	5/2011	Poupyrev et al.
7,973,772	B2	7/2011	Gettemy et al.
7,973,778	B2	7/2011	Chen
8,004,052	B2	8/2011	Vaganov
8,004,501	B2	8/2011	Harrison
8,013,843	B2	9/2011	Pryor
8,026,906	B2	9/2011	Mölne et al.
8,044,929	B2	10/2011	Baldo et al.
3,051,705	A1	11/2011	Kobayakawa
8,068,100	B2	11/2011	Pryor
8,072,437	B2	12/2011	Miller et al.
8,072,440	B2	12/2011	Pryor
8,096,188	B2	1/2012	Wilner
8,113,065	B2	2/2012	Ohsato et al.
8,120,586	B2	2/2012	Hsu et al.
8,120,588	B2	2/2012	Klinghult
8,130,207	B2	3/2012	Nurmi et al.
8,134,535	B2	3/2012	Choi et al.
8,139,038	B2	3/2012	Chueh et al.
8,144,133	B2	3/2012	Wang et al.
8,149,211	B2	4/2012	Hayakawa et al.
8,154,528	B2	4/2012	Chen et al.
8,159,473	B2	4/2012	Cheng et al.
8,164,573	B2	4/2012	DaCosta et al.
8,183,077	B2	5/2012	Vaganov et al.
8,184,093	B2	5/2012	Tsuiki
8,188,985	B2	5/2012	Hillis et al.
8,196,477	B2	6/2012	Ohsato et al.
8,199,116	B2	6/2012	Jeon et al.
8,212,790	B2	7/2012	Rimas-Ribikauskas et al.
8,220,330	B2 *	7/2012	Miller G01P 15/0802 73/514.32
8,237,537	B2	8/2012	Kurtz et al.
8,243,035	B2	8/2012	Abe et al.
8,250,921	B2	8/2012	Nasiri et al.
8,253,699	B2	8/2012	Son
8,260,337	B2	9/2012	Periyalwar et al.
8,269,731	B2	9/2012	Mölne
8,289,288	B2	10/2012	Whytock et al.
8,289,290	B2	10/2012	Klinghult
8,297,127	B2	10/2012	Wade et al.
8,316,533	B2	11/2012	Suminto et al.

(56) **References Cited**

U.S. PATENT DOCUMENTS

8,319,739 B2 11/2012 Chu et al.
8,325,143 B2 12/2012 Destura et al.
8,350,345 B2 1/2013 Vaganov
8,363,020 B2 1/2013 Li et al.
8,363,022 B2 1/2013 Tho et al.
8,378,798 B2 2/2013 Bells et al.
8,378,991 B2 2/2013 Jeon et al.
8,384,677 B2 2/2013 Mak-Fan et al.
8,387,464 B2 3/2013 McNeil et al.
8,405,631 B2 3/2013 Chu et al.
8,405,632 B2 3/2013 Chu et al.
8,421,609 B2 4/2013 Kim et al.
8,427,441 B2 4/2013 Paleczny et al.
8,436,806 B2 5/2013 Almalki et al.
8,436,827 B1 5/2013 Zhai et al.
8,448,531 B2 5/2013 Schneider
8,451,245 B2 5/2013 Heubel et al.
8,456,440 B2 6/2013 Abe et al.
8,466,889 B2 6/2013 Tong et al.
8,477,115 B2 7/2013 Rekimoto
8,482,372 B2 7/2013 Kurtz et al.
8,493,189 B2 7/2013 Suzuki
8,497,757 B2 7/2013 Kurtz et al.
8,516,906 B2 8/2013 Umetsu et al.
8,646,335 B2 * 2/2014 Kotovsky G01L 1/18 73/777
8,833,172 B2 * 9/2014 Chiou G01L 9/0054 73/708
8,931,347 B2 1/2015 Donzier et al.
8,973,446 B2 3/2015 Fukuzawa et al.
8,984,951 B2 3/2015 Landmann et al.
8,991,265 B2 3/2015 Dekker et al.
9,032,818 B2 5/2015 Campbell et al.
9,097,600 B2 8/2015 Khandani
9,143,057 B1 9/2015 Shah et al.
9,182,302 B2 11/2015 Lim et al.
9,366,588 B2 6/2016 Lee
9,377,372 B2 6/2016 Ogawa
9,425,328 B2 8/2016 Marx et al.
9,446,944 B2 9/2016 Ernst et al.
9,464,952 B2 10/2016 Pagani et al.
9,487,388 B2 11/2016 Brosh
9,493,342 B2 11/2016 Brosh
9,574,954 B2 2/2017 Baker et al.
9,709,509 B1 7/2017 Yang
9,728,652 B2 8/2017 Elian et al.
9,772,245 B2 9/2017 Besling et al.
9,778,117 B2 10/2017 Pagani
9,791,303 B2 10/2017 Pagani et al.
9,823,144 B2 11/2017 Fujisawa et al.
9,835,515 B2 12/2017 Pagani
9,846,091 B2 12/2017 Lu et al.
9,851,266 B2 12/2017 Nakamura et al.
9,970,831 B2 5/2018 Shih
9,983,084 B2 5/2018 Pavone
10,024,738 B2 7/2018 Conti et al.
10,067,014 B1 9/2018 Tung et al.
10,113,925 B2 10/2018 Lai et al.
10,488,284 B2 11/2019 Jentoft et al.
10,496,209 B2 12/2019 Vummidi Murali et al.
10,598,578 B2 3/2020 Pagani et al.
10,724,909 B2 7/2020 Abbasi Gavarti et al.
10,962,427 B2 3/2021 Youssef et al.
11,385,108 B2 * 7/2022 Tsai G01L 1/18
2001/0009112 A1 7/2001 Delaye
2003/0067448 A1 4/2003 Park
2003/0128181 A1 7/2003 Poole
2003/0189552 A1 10/2003 Chuang et al.
2004/0012572 A1 1/2004 Sowden et al.
2004/0140966 A1 7/2004 Marggraff et al.
2005/0083310 A1 4/2005 Safai et al.
2005/0166687 A1 8/2005 Kaneko et al.
2005/0190152 A1 9/2005 Vaganov
2006/0028441 A1 2/2006 Armstrong
2006/0244733 A1 11/2006 Geaghan
2006/0272413 A1 12/2006 Vaganov et al.
2006/0284856 A1 12/2006 Soss
2007/0035525 A1 2/2007 Yeh et al.
2007/0046649 A1 3/2007 Reiner
2007/0070046 A1 3/2007 Sheynblat et al.
2007/0070053 A1 3/2007 Lapstun et al.
2007/0097095 A1 5/2007 Kim et al.
2007/0103449 A1 5/2007 Laitinen et al.
2007/0103452 A1 5/2007 Wakai et al.
2007/0115265 A1 5/2007 Rainisto
2007/0132717 A1 6/2007 Wang et al.
2007/0137901 A1 6/2007 Chen
2007/0139391 A1 6/2007 Bischoff
2007/0152959 A1 7/2007 Peters
2007/0156723 A1 7/2007 Vaananen
2007/0182864 A1 8/2007 Stoneham et al.
2007/0229478 A1 10/2007 Rosenberg et al.
2007/0235231 A1 10/2007 Loomis et al.
2007/0245836 A1 10/2007 Vaganov
2007/0262965 A1 11/2007 Hirai et al.
2007/0277616 A1 12/2007 Nikkel et al.
2007/0298883 A1 12/2007 Feldman et al.
2008/0001923 A1 1/2008 Hall et al.
2008/0007532 A1 1/2008 Chen
2008/0010616 A1 1/2008 Algreatly
2008/0024454 A1 1/2008 Everest
2008/0030482 A1 2/2008 Elwell et al.
2008/0036743 A1 2/2008 Westerman et al.
2008/0083962 A1 4/2008 Vaganov
2008/0088600 A1 4/2008 Prest et al.
2008/0088602 A1 4/2008 Hotelling
2008/0094367 A1 4/2008 Van De Ven et al.
2008/0105057 A1 5/2008 Wade
2008/0105470 A1 5/2008 Van De Ven et al.
2008/0106523 A1 5/2008 Conrad
2008/0174852 A1 7/2008 Hirai et al.
2008/0180402 A1 7/2008 Yoo et al.
2008/0180405 A1 7/2008 Han et al.
2008/0180406 A1 7/2008 Han et al.
2008/0202249 A1 8/2008 Yokura et al.
2008/0204427 A1 8/2008 Heesemans et al.
2008/0211766 A1 9/2008 Westerman et al.
2008/0238446 A1 10/2008 DeNatale et al.
2008/0238884 A1 10/2008 Harish
2008/0259046 A1 10/2008 Carsanaro
2008/0284742 A1 11/2008 Prest et al.
2008/0303799 A1 12/2008 Schwesig et al.
2009/0027352 A1 1/2009 Abele
2009/0027353 A1 1/2009 Im et al.
2009/0046110 A1 2/2009 Sadler et al.
2009/0078040 A1 3/2009 Ike et al.
2009/0102805 A1 4/2009 Meijer et al.
2009/0140985 A1 6/2009 Liu
2009/0184921 A1 7/2009 Scott et al.
2009/0184936 A1 7/2009 Algreatly
2009/0213066 A1 8/2009 Hardacker et al.
2009/0237275 A1 9/2009 Vaganov
2009/0237374 A1 9/2009 Li et al.
2009/0242282 A1 10/2009 Kim et al.
2009/0243817 A1 10/2009 Son
2009/0243998 A1 10/2009 Wang
2009/0256807 A1 10/2009 Nurmi
2009/0256817 A1 10/2009 Perlin et al.
2009/0282930 A1 11/2009 Cheng et al.
2009/0303400 A1 12/2009 Hou et al.
2009/0309852 A1 12/2009 Lin et al.
2009/0314551 A1 12/2009 Nakajima
2010/0013785 A1 1/2010 Murai et al.
2010/0020030 A1 1/2010 Kim et al.
2010/0020039 A1 1/2010 Ricks et al.
2010/0039396 A1 2/2010 Ho et al.
2010/0053087 A1 3/2010 Dai et al.
2010/0053116 A1 3/2010 Daverman et al.
2010/0066686 A1 3/2010 Joguet et al.
2010/0066697 A1 3/2010 Jacomet et al.
2010/0079391 A1 4/2010 Joung
2010/0079395 A1 4/2010 Kim et al.
2010/0079398 A1 4/2010 Shen et al.
2010/0097347 A1 4/2010 Lin

(56) **References Cited**

U.S. PATENT DOCUMENTS

2010/0102403 A1 4/2010 Celik-Butler et al.
2010/0117978 A1 5/2010 Shirado
2010/0123671 A1 5/2010 Lee
2010/0123686 A1 5/2010 Klinghult et al.
2010/0127140 A1 5/2010 Smith
2010/0128002 A1 5/2010 Stacy et al.
2010/0153891 A1 6/2010 Vaananen et al.
2010/0164959 A1 7/2010 Brown et al.
2010/0220065 A1 9/2010 Ma
2010/0224004 A1 9/2010 Suminto et al.
2010/0271325 A1 10/2010 Conte et al.
2010/0289807 A1 11/2010 Yu et al.
2010/0295807 A1 11/2010 Xie et al.
2010/0308844 A1 12/2010 Day et al.
2010/0309714 A1 12/2010 Meade
2010/0315373 A1 12/2010 Steinhauser et al.
2010/0321310 A1 12/2010 Kim et al.
2010/0321319 A1 12/2010 Hefti et al.
2010/0323467 A1 12/2010 Vaganov et al.
2010/0328229 A1 12/2010 Weber et al.
2010/0328230 A1 12/2010 Faubert et al.
2011/0001723 A1 1/2011 Fan
2011/0006980 A1 1/2011 Taniguchi et al.
2011/0007008 A1 1/2011 Algreatly
2011/0012848 A1 1/2011 Li et al.
2011/0018820 A1 1/2011 Huitema et al.
2011/0032211 A1 2/2011 Christoffersen
2011/0039602 A1 2/2011 McNamara et al.
2011/0050628 A1 3/2011 Homma et al.
2011/0050630 A1 3/2011 Ikeda
2011/0057899 A1 3/2011 Sleeman et al.
2011/0063248 A1 3/2011 Yoon
2011/0113881 A1 5/2011 Suzuki
2011/0128250 A1 6/2011 Murphy et al.
2011/0141052 A1 6/2011 Bernstein et al.
2011/0141053 A1 6/2011 Bulea et al.
2011/0187674 A1 8/2011 Baker et al.
2011/0209555 A1 9/2011 Ahles et al.
2011/0227836 A1 9/2011 Li et al.
2011/0242014 A1 10/2011 Tsai et al.
2011/0267181 A1 11/2011 Kildal
2011/0267294 A1 11/2011 Kildal
2011/0273396 A1 11/2011 Chung
2011/0291951 A1 12/2011 Tong
2011/0298705 A1 12/2011 Vaganov
2011/0308324 A1 12/2011 Gamage et al.
2012/0025337 A1* 2/2012 LeClair B81B 7/0048
257/419
2012/0032907 A1 2/2012 Koizumi et al.
2012/0032915 A1 2/2012 Wittorf
2012/0038579 A1 2/2012 Sasaki
2012/0044169 A1 2/2012 Enami
2012/0044172 A1 2/2012 Ohki et al.
2012/0050159 A1 3/2012 Yu et al.
2012/0050208 A1 3/2012 Dietz
2012/0056837 A1 3/2012 Park et al.
2012/0060605 A1 3/2012 Wu et al.
2012/0061823 A1 3/2012 Wu et al.
2012/0062603 A1 3/2012 Mizunuma et al.
2012/0068946 A1 3/2012 Tang et al.
2012/0068969 A1 3/2012 Bogana et al.
2012/0081327 A1 4/2012 Heubel et al.
2012/0086659 A1 4/2012 Perlin et al.
2012/0092250 A1 4/2012 Hadas et al.
2012/0092279 A1 4/2012 Martin
2012/0092294 A1 4/2012 Ganapathi et al.
2012/0092299 A1 4/2012 Harada et al.
2012/0092324 A1 4/2012 Buchan et al.
2012/0105358 A1 5/2012 Momeyer et al.
2012/0105367 A1 5/2012 Son et al.
2012/0113061 A1 5/2012 Ikeda
2012/0127088 A1 5/2012 Pance et al.
2012/0127107 A1 5/2012 Miyashita et al.
2012/0139864 A1 6/2012 Sleeman et al.
2012/0144921 A1 6/2012 Bradley et al.
2012/0146945 A1 6/2012 Miyazawa et al.
2012/0146946 A1 6/2012 Wang et al.
2012/0147052 A1 6/2012 Homma et al.
2012/0154315 A1 6/2012 Aono
2012/0154316 A1 6/2012 Kono
2012/0154317 A1 6/2012 Aono
2012/0154318 A1 6/2012 Aono
2012/0154328 A1 6/2012 Kono
2012/0154329 A1 6/2012 Shinozaki
2012/0154330 A1 6/2012 Shimizu
2012/0162122 A1 6/2012 Geaghan
2012/0169609 A1 7/2012 Britton
2012/0169617 A1 7/2012 Mäenpää
2012/0169635 A1 7/2012 Liu
2012/0169636 A1 7/2012 Liu
2012/0180575 A1 7/2012 Sakano et al.
2012/0188181 A1 7/2012 Ha et al.
2012/0194460 A1 8/2012 Kuwabara et al.
2012/0194466 A1 8/2012 Posamentier
2012/0200526 A1 8/2012 Lackey
2012/0204653 A1 8/2012 August et al.
2012/0205165 A1 8/2012 Strittmatter et al.
2012/0218212 A1 8/2012 Yu et al.
2012/0234112 A1 9/2012 Umetsu et al.
2012/0256237 A1 10/2012 Lakamraju et al.
2012/0286379 A1 11/2012 Inoue
2012/0319987 A1 12/2012 Woo
2012/0327025 A1 12/2012 Huska et al.
2013/0008263 A1 1/2013 Kabasawa et al.
2013/0038541 A1 2/2013 Bakker
2013/0093685 A1 4/2013 Kalu et al.
2013/0096849 A1 4/2013 Campbell et al.
2013/0140944 A1 6/2013 Chen et al.
2013/0187201 A1 7/2013 Elian et al.
2013/0239700 A1 9/2013 Benfield et al.
2013/0255393 A1 10/2013 Fukuzawa et al.
2013/0341741 A1 12/2013 Brosh
2013/0341742 A1 12/2013 Brosh
2014/0007705 A1 1/2014 Campbell et al.
2014/0028575 A1 1/2014 Parivar et al.
2014/0055407 A1 2/2014 Lee et al.
2014/0090488 A1 4/2014 Taylor et al.
2014/0109693 A1 4/2014 Sakai
2014/0230563 A1 8/2014 Huang
2014/0260678 A1 9/2014 Jentoft et al.
2014/0283604 A1 9/2014 Najafi et al.
2014/0367811 A1 12/2014 Nakagawa et al.
2015/0110295 A1 4/2015 Jenkner et al.
2015/0226618 A1 8/2015 Shih
2015/0241465 A1 8/2015 Konishi
2015/0362389 A1 12/2015 Yanev et al.
2016/0069927 A1 3/2016 Hamamura
2016/0103545 A1* 4/2016 Filiz G01L 1/005
345/174
2016/0245667 A1 8/2016 Najafi et al.
2016/0332866 A1 11/2016 Brosh et al.
2016/0354589 A1 12/2016 Kobayashi et al.
2016/0363490 A1 12/2016 Campbell et al.
2017/0103246 A1 4/2017 Pi et al.
2017/0205303 A1 7/2017 Sanden et al.
2017/0233245 A1 8/2017 Duqi et al.
2017/0234744 A1 8/2017 Tung et al.
2018/0058914 A1 3/2018 Iesato
2018/0058955 A1 3/2018 Wade et al.
2019/0330053 A1 10/2019 Tseng et al.
2019/0383675 A1 12/2019 Tsai et al.
2019/0383676 A1 12/2019 Foughi et al.
2020/0149983 A1 5/2020 Tsai et al.
2020/0234023 A1 7/2020 Tsai et al.
2020/0309615 A1 10/2020 Tsai et al.

FOREIGN PATENT DOCUMENTS

CN 101801837 A 8/2010
CN 201653605 11/2010
CN 101929898 A 12/2010
CN 102062662 A 5/2011
CN 102853950 A 1/2013
CN 102998037 3/2013

(56) **References Cited**

FOREIGN PATENT DOCUMENTS

CN	103308239	A	9/2013
CN	104535229	A	4/2015
CN	104581605	A	4/2015
CN	104919293	A	9/2015
CN	105934661	A	9/2016
DE	102010012441		9/2011
JP	2004-156937		6/2004
JP	2010147268		7/2010
WO	9310430	A1	5/1993
WO	2004/113859		12/2004
WO	2007/139695		12/2007
WO	2011065250	A1	6/2011
WO	2013/067548		5/2013
WO	2015/039811	B1	3/2015
WO	2015106246	A1	7/2015
WO	2018148503	A1	8/2018
WO	2018148510	A1	8/2018
WO	2019023552	A1	1/2019
WO	2019079420	A1	4/2019

OTHER PUBLICATIONS

PCT/US2018/056245, International Search Report and Written Opinion, dated Dec. 27, 2018.

Mei, T., et al., "Design and Fabrication of an Integrated Three-Dimensional Tactile Sensor for Space Robotic Applications," Micro Electro Mechanical Systems, MEMS '99, Twelfth IEEE International Conference, Orlando Florida, Jan. 21, 1999, pp. 112-117.

Nesterov, V., et al., "Modelling and investigation of the silicon twin design 3D micro probe," Journal of Micromechanics and Microengineering, vol. 15, 2005, pp. 514-520.

Non-Final Office Action for U.S. Appl. No. 16/485,016, dated Jun. 12, 2020, 13 pages.

Final Office Action for U.S. Appl. No. 16/485,016, dated Mar. 24, 2021, 10 pages.

Notice of Allowance for U.S. Appl. No. 16/485,016, dated Jul. 9, 2021, 8 pages.

Non-Final Office Action for U.S. Appl. No. 16/485,026, dated Apr. 28, 2021, 13 pages.

Applicant-Initiated Interview Summary for U.S. Appl. No. 16/485,026, dated Aug. 25, 2021, 2 pages.

Notice of Allowance for U.S. Appl. No. 16/485,026, dated Sep. 30, 2021, 8 pages.

Non-Final Office Action for U.S. Appl. No. 16/632,795, dated Feb. 18, 2021, 10 pages.

Non-Final Office Action for U.S. Appl. No. 16/634,469, dated May 27, 2021, 13 pages.

Notice of Allowance for U.S. Appl. No. 16/634,469, dated Sep. 30, 2021, 8 pages.

Non-Final Office Action for U.S. Appl. No. 16/764,992, dated Jun. 24, 2021, 15 pages.

Final Office Action for U.S. Appl. No. 16/764,992, dated Jan. 19, 2022, 15 pages.

Advisory Action, Examiner-Initiated Interview Summary, and AFCP 2.0 Decision for U.S. Appl. No. 16/764,992, dated Apr. 20, 2022, 5 pages.

First Office Action for Chinese Patent Application No. 201880023913.1, dated Dec. 25, 2020, 22 pages.

Second Office Action for Chinese Patent Application No. 201880023913.1, dated Sep. 10, 2021, 13 pages.

Third Office Action for Chinese Patent Application No. 201880023913.1, dated Apr. 6, 2022, 13 pages.

Extended European Search Report for European Patent Application No. 18751209.0, dated Oct. 22, 2020, 7 pages.

International Search Report and Written Opinion for International Patent Application No. PCT/US2018/017564, dated Jun. 15, 2018, 10 pages.

International Search Report and Written Opinion for International Patent Application No. PCT/US2018/017572, dated May 3, 2018, 8 pages.

International Search Report and Written Opinion for International Patent Application No. PCT/US2018/056245, dated Dec. 27, 2018, 8 pages.

Office Action for Chinese Patent Application No. 2018800601531, dated Apr. 6, 2021, 16 pages.

Communication Pursuant to Rule 164(1) EPC issued for European Application No. 18834426.1, dated Mar. 10, 2021, 16 pages.

Extended European Search Report issued for European Application No. 18834426.1, dated Jun. 10, 2021, 13 pages.

International Search Report and Written Opinion for International Patent Application No. PCT/US2018/042883, dated Dec. 6, 2018, 9 pages.

International Search Report and Written Opinion for International Patent Application No. PCT/US2018/044049, dated Oct. 18, 2018, 11 pages.

PCT/US2018/061509, International Search Report and Written Opinion of the International Searching Authority, dated Jan. 29, 2019, 8 pages.

Notice of Allowance for U.S. Appl. No. 16/632,795, dated Sep. 3, 2021, 7 pages.

Non-Final Office Action for U.S. Appl. No. 16/764,992, dated Jun. 14, 2022, 14 pages.

Final Office Action for U.S. Appl. No. 16/764,992, dated Jan. 6, 2023, 13 pages.

Decision of Rejection for Chinese Patent Application No. 201880023913.1, dated Oct. 27, 2022, 9 pages.

Non-Final Office Action for U.S. Appl. No. 17/676,477, dated Nov. 23, 2022, 12 pages.

Notice of Allowance for U.S. Appl. No. 17/51,715, dated Oct. 26, 2022, 13 pages.

Notice of Allowance for U.S. Appl. No. 17/591,706, dated Nov. 10, 2022, 12 pages.

* cited by examiner

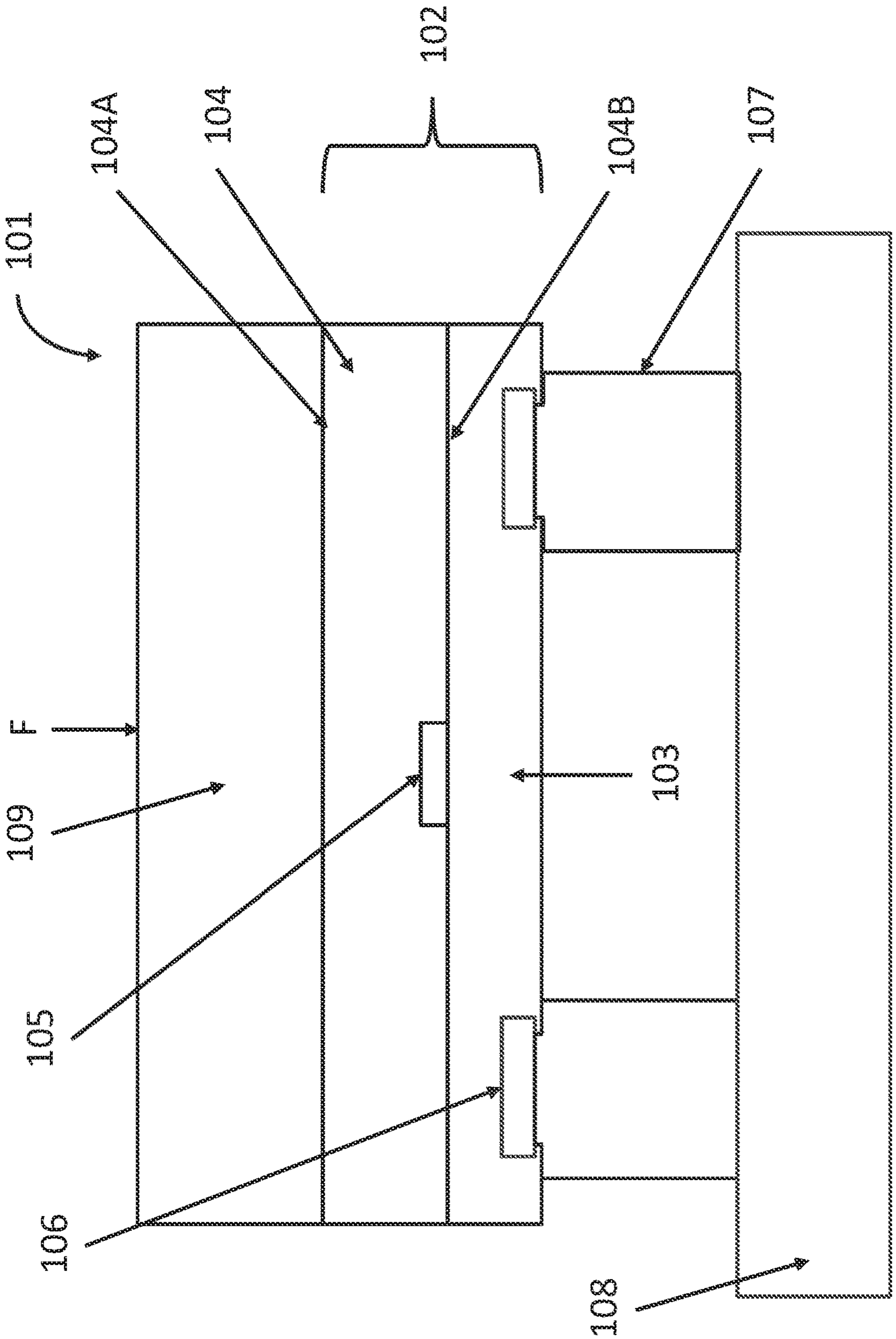

FIG. 1

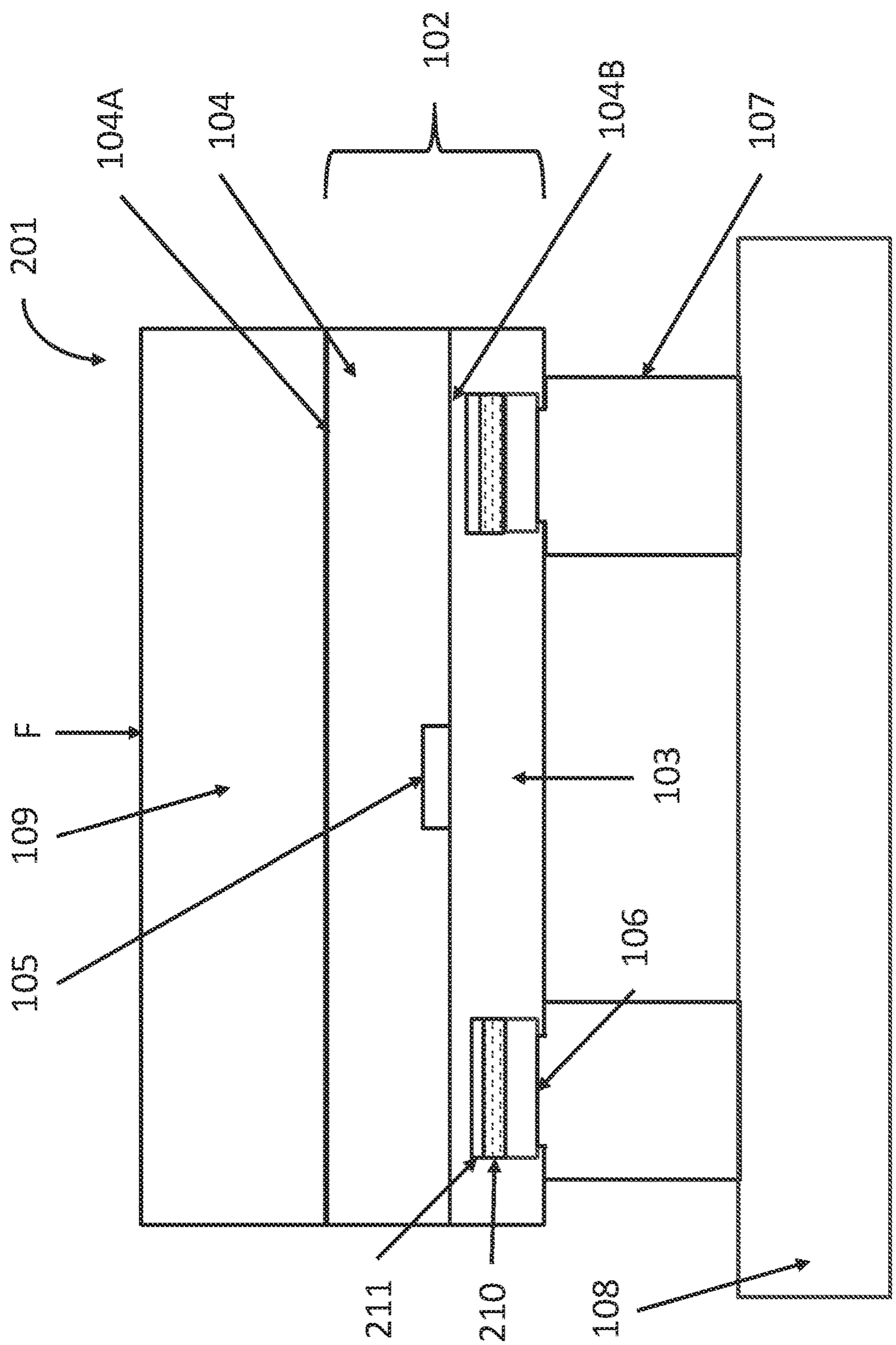

FIG. 2

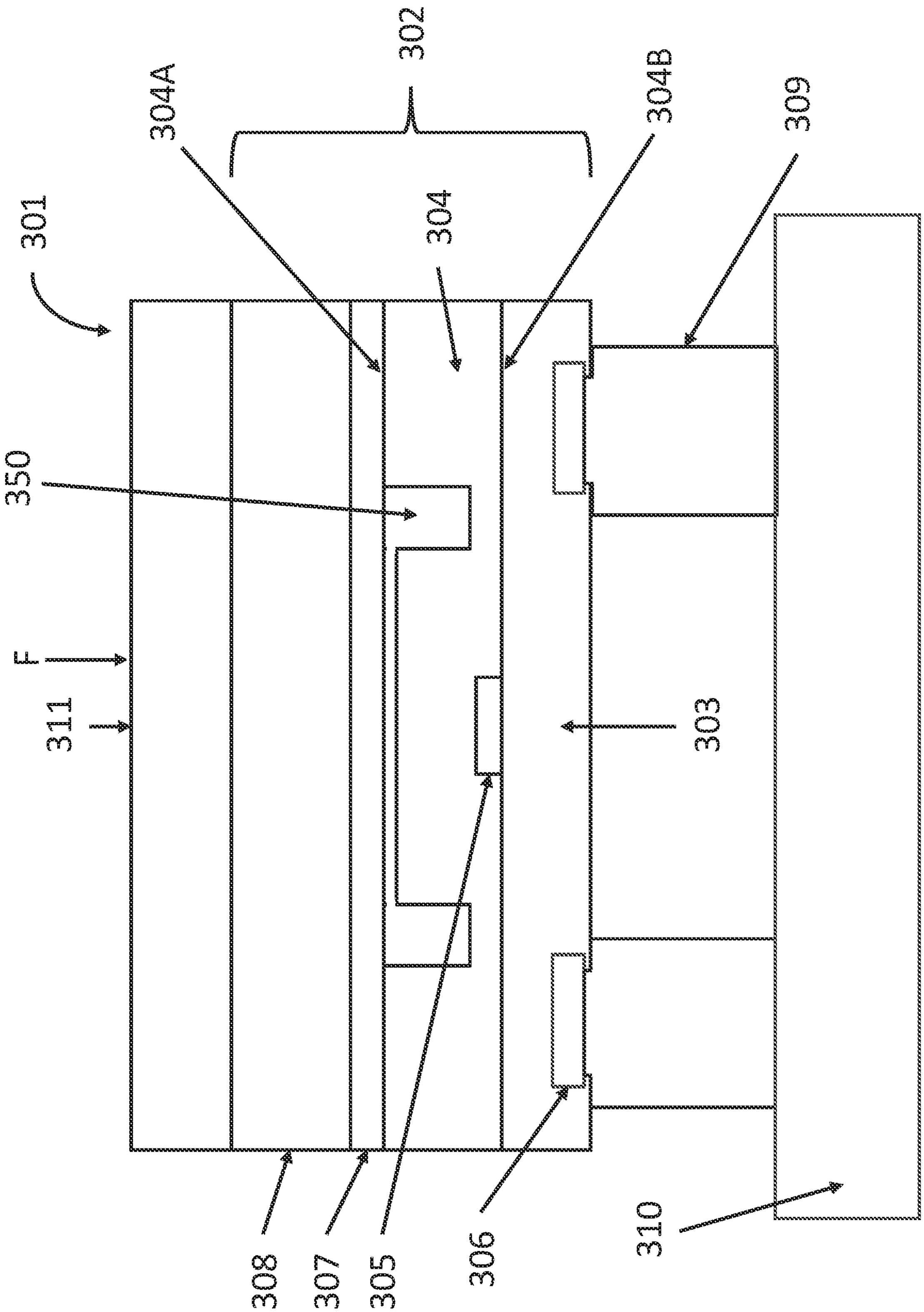

FIG. 3

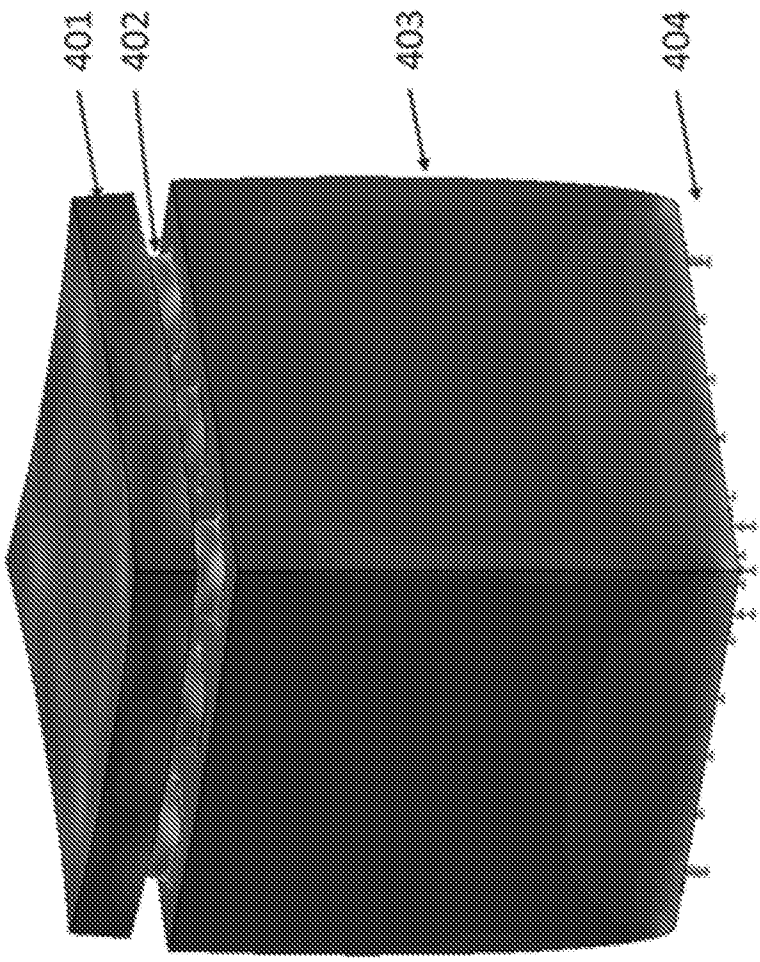

FIG. 4

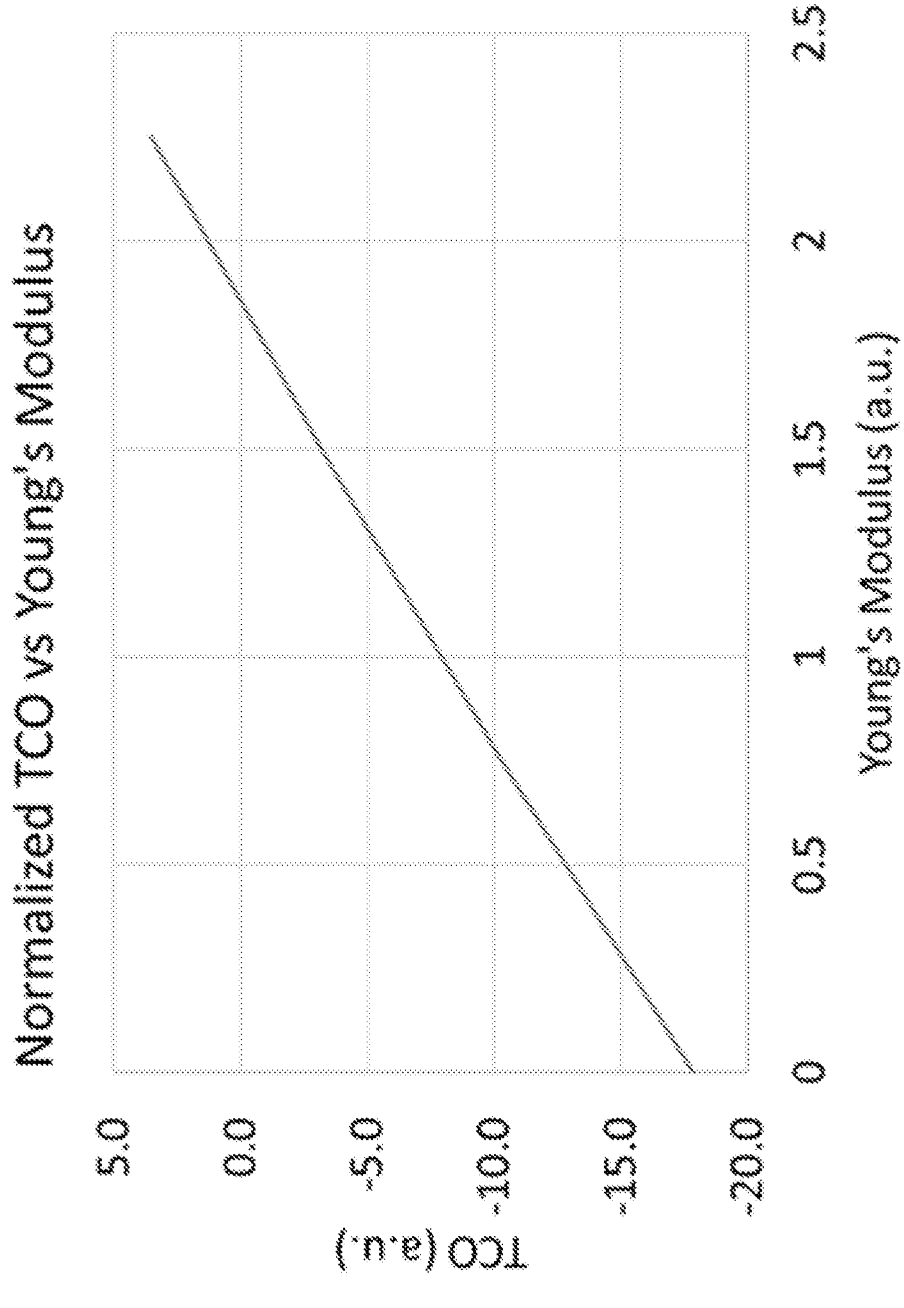
Normalized TCO vs Young's Modulus
TCO (a.u.)
5.0
0.0
-5.0
-10.0
-15.0
-20.0
0
0.5
1
1.5
2
2.5
Young's Modulus (a.u.)

FIG. 5

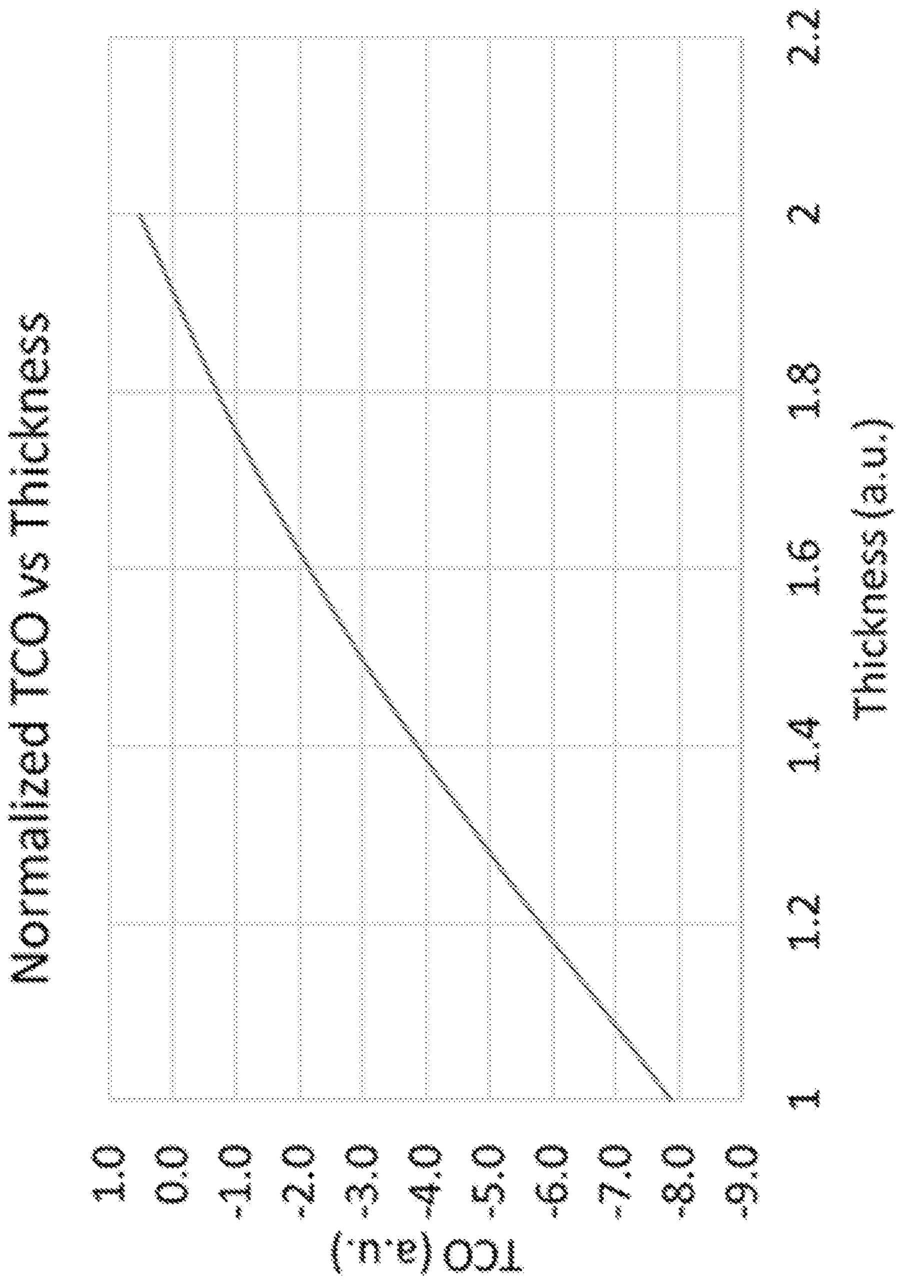
Normalized TCO vs Thickness
TCO (a.u.)
1.0
0.0
-1.0
-2.0
-3.0
-4.0
-5.0
-6.0
-7.0
-8.0
-9.0
Thickness (a.u.)
1
1.2
1.4
1.6
1.8
2
2.2

FIG. 6

TEMPERATURE COEFFICIENT OF OFFSET COMPENSATION FOR FORCE SENSOR AND STRAIN GAUGE

CROSS-REFERENCE TO RELATED APPLICATIONS

This application is a national stage application filed under 35 U.S.C. § 371 of PCT/US2018/056245 filed Oct. 17, 2018, which claims the benefit of U.S. provisional patent application No. 62/573,271, filed on Oct. 17, 2017, and entitled "TCO COMPENSATION FOR FORCE SENSOR AND STRAIN GAUGE," the disclosures of which are expressly incorporated herein by reference in their entireties.

FIELD OF TECHNOLOGY

The present disclosure relates to temperature coefficient of offset (TCO) compensation for force sensors and strain gauges in the chip scale package format.

BACKGROUND

A MEMS force sensor or strain gauge has intrinsic offset as a result of the manufacturing and assembly processes. Additionally, the offset of the sensor can change in relation to temperature due to the thermal coefficient of expansion (TCE) mismatch between the package substrate, substrate of the sensor, solder bumps, and/or inter metal dielectric layers of the sensor chip. The slope of the offset versus temperature is defined as the temperature coefficient of offset (TCO). The offset under extreme temperatures can put subsequent amplifier and/or analog-to-digital convertor out of normal operation range and thus render the entire sensing system unusable.

In some conventional systems, the solution to TCO problems involve the electrical sensing circuitry, which broadens the operation range of the MEMS force sensor.

SUMMARY

According to the present disclosure, a TCO compensation layer is provided on the MEMS force sensor to minimize the offset drift over temperature. By choosing the right combination of Young's modulus, thickness, and TCE, the TCO of the MEMS force sensor can be reduced to zero.

An example microelectromechanical ("MEMS") force sensor for providing temperature coefficient of offset (TCO) compensation is described herein. The force sensor can include a sensor substrate configured to receive an applied force, where the sensor substrate can include a top surface and a bottom surface opposite thereto. The force sensor can also include a sensing element arranged on the bottom surface of the sensor substrate, where the sensing element is configured to convert a strain on the bottom surface of the sensor substrate to an electrical signal that is proportional to the strain. The force sensor can further include a compensation layer arranged on the top surface of the sensor substrate, where the compensation layer has a thermal coefficient of expansion that is different than a thermal coefficient of expansion of the sensor substrate.

Additionally, the thermal coefficient of expansion of the compensation layer can be less than the thermal coefficient of expansion of the sensor substrate. Alternatively, the thermal coefficient of expansion of the compensation layer can be greater than the thermal coefficient of expansion of the sensor substrate.

Alternatively or additionally, the thermal coefficient of expansion of the compensation layer can be within the same order of magnitude of a thermal coefficient of expansion of a package substrate.

Alternatively or additionally, at least one of a thickness of the compensation layer, a stiffness of the compensation layer, and/or the thermal coefficient of expansion of the compensation layer can minimize TCO. Optionally, a combination of a thickness, a stiffness, and the thermal coefficient of expansion of the compensation layer of the compensation layer can minimize TCO. Optionally, TCO is minimized at a value of about zero.

Alternatively or additionally, the MEMS force sensor can be configured for use as strain gauge.

Alternatively or additionally, the sensing element can be a piezoresistive sensing element.

Alternatively or additionally, the sensing element can be piezoresistive and piezoelectric elements.

Alternatively or additionally, the force sensor can further include a cap substrate, where the sensor and cap substrates are bonded together forming a sealed cavity there between.

Alternatively or additionally, the force sensor can be configured for electrical and mechanical coupling to a package substrate. In some implementations, the force sensor can be electrically and mechanically coupled to the package substrate. The package substrate can be a printed circuit board (PCB), a flexible printed circuit board (FPC), or a co-fired ceramic.

Alternatively or additionally, the compensation layer can be formed of at least one of polymer, polyimide, resin, polycarbonate, acrylonitrile butadiene styrene (ABS), silicon oxide, glass, or combinations thereof.

Alternatively or additionally, the force sensor can further include a plurality of sensing elements arranged on the bottom surface of the sensor substrate.

Other systems, methods, features and/or advantages will be or may become apparent to one with skill in the art upon examination of the following drawings and detailed description. It is intended that all such additional systems, methods, features and/or advantages be included within this description and be protected by the accompanying claims.

BRIEF DESCRIPTION OF THE DRAWINGS

The components in the drawings are not necessarily to scale relative to each other. Like reference numerals designate corresponding parts throughout the several views.

FIG. **1** illustrates a MEMS force sensor using piezoresistive sensing element(s) with the TCO compensation layer. As shown in FIG. **1**, the MEMS force sensor is mounted on a package substrate through solder bumps.

FIG. **2** illustrates a MEMS force sensor using both piezoresistive and piezoelectric sensing element(s) with the TCO compensation layer. As shown in FIG. **2**, the MEMS force sensor is mounted on a package substrate through solder bumps.

FIG. **3** illustrates a MEMS force sensor having a sealed cavity and using piezoresistive sensing element(s) with the TCO compensation layer. As shown in FIG. **3**, the MEMS force sensor is mounted on a package substrate through solder bumps.

FIG. **4** illustrates an exaggerated deformation due to a temperature increase from a zero stress condition.

FIG. **5** illustrates normalized TCO with fixed TCO compensation layer thickness and TCE versus the Young's modulus of the TCO compensation layer.

FIG. 6 illustrates normalized TCO with fixed TCO compensation layer Young's modulus and TCE versus the TCO compensation layer thickness.

DETAILED DESCRIPTION

The present disclosure can be understood more readily by reference to the following detailed description, examples, drawings, and their previous and following description. However, before the present devices, systems, and/or methods are disclosed and described, it is to be understood that this disclosure is not limited to the specific devices, systems, and/or methods disclosed unless otherwise specified, and, as such, can, of course, vary. It is also to be understood that the terminology used herein is for the purpose of describing particular aspects only and is not intended to be limiting.

The following description is provided as an enabling teaching. To this end, those skilled in the relevant art will recognize and appreciate that many changes can be made, while still obtaining beneficial results. It will also be apparent that some of the desired benefits can be obtained by selecting some of the features without utilizing other features. Accordingly, those who work in the art will recognize that many modifications and adaptations may be possible and can even be desirable in certain circumstances, and are contemplated by this disclosure. Thus, the following description is provided as illustrative of the principles and not in limitation thereof.

As used throughout, the singular forms "a," "an" and "the" include plural referents unless the context clearly dictates otherwise. Thus, for example, reference to "a force sensing element" can include two or more such force sensing elements unless the context indicates otherwise.

The term "comprising" and variations thereof as used herein is used synonymously with the term "including" and variations thereof and are open, non-limiting terms.

Ranges can be expressed herein as from "about" one particular value, and/or to "about" another particular value. When such a range is expressed, another aspect includes from the one particular value and/or to the other particular value. Similarly, when values are expressed as approximations, by use of the antecedent "about," it will be understood that the particular value forms another aspect. It will be further understood that the endpoints of each of the ranges are significant both in relation to the other endpoint, and independently of the other endpoint.

As used herein, the terms "optional" or "optionally" mean that the subsequently described event or circumstance may or may not occur, and that the description includes instances where said event or circumstance occurs and instances where it does not.

The present disclosure relates to the TCO compensation layer for MEMS force sensor and strain gauge. Three different types of MEMS force sensor's TCO can be compensated with this layer. The force sensor can also be reconfigured as strain gauge if the force is applied through the package substrate. The root cause of the TCO is illustrated and the material property and dimension effect to the TCO is also illustrated.

FIG. **1** illustrates the force sensor **102** (e.g., a MEMS force sensor) mounted on a package substrate **108**. The package substrate **108** can be a printed circuit board (PCB), a flexible printed circuit board (FPC), or a co-fired ceramic. It should be understood that PCBs, FPCs, and co-fired ceramics are provided only as example package substrates. The combined force sensor and package substrate is shown by reference number **101** in FIG. **1**. The force sensor **102** can include a dielectric layer **103**, a sensor substrate **104**, and a piezoresistive sensing element **105**. The sensor substrate, which can also be referred to as a sensor die, can be made of a semiconductor material such as silicon or gallium arsenide, for example. As shown in FIG. **1**, the sensor substrate **104** has a top surface **104**A and a bottom surface **104**B, which is opposite to the top surface **104**A. The piezoresistive sensing element **105** is arranged on the bottom surface **104**B. Optionally, in some implementations, a plurality of piezoresistive sensing elements **105** can be arranged on the sensor substrate **104**. This disclosure contemplates that the piezoresistive sensing element(s) **105** can be diffused, deposited, or implanted on the bottom surface **104**B. The dielectric layer **103** can then be arranged (e.g., deposited) over the bottom surface **104**B to electrically isolate the piezoresistive sensing element(s) **105**.

The piezoresistive sensing element **105** can change an electrical characteristic (e.g., resistance) in response to deflection of the sensor substrate **104**. For example, the piezoresistive sensing element **105** can sense strain on the bottom surface **104**A of the sensor substrate **104**. The change in electrical characteristic can be measured as an analog electrical signal. In one implementation, the piezoresistive sensing element **105** can optionally be a piezoresistive transducer. For example, as strain is induced in the sensor substrate **104** proportional to a force "F" applied to the force sensor **102**, a localized strain is produced on the piezoresistive transducer such that the piezoresistive transducer experiences compression or tension, depending on its specific orientation. As the piezoresistive transducer compresses and tenses, its resistivity changes in opposite fashion. Accordingly, a Wheatstone bridge circuit including a plurality (e.g., four) piezoresistive transducers (e.g., two of each orientation relative to strain) becomes unbalanced and produces a differential voltage (also sometimes referred to herein as an "analog electrical signal") across the positive signal terminal and the negative signal terminal. This differential voltage is directly proportional to the applied force "F" on the force sensor **102**. This differential voltage can be received at and processed by digital circuitry. For example, digital circuitry can be configured to, among other functions, convert the analog electrical signal to a digital electrical signal. Although piezoresistive transducers are provided as an example sensing element, this disclosure contemplates that the sensing element(s) can be any sensor element configured to change at least one electrical characteristic (e.g., resistance, charge, capacitance, etc.) based on an amount or magnitude of an applied force and can output a signal proportional to the amount or magnitude of the applied force. Other types of sensing elements include, but are not limited to, piezoelectric or capacitive sensors. Additionally, application of force "F" to the force sensor **102** is provided only as an example. This disclosure contemplates that force can be applied to other sides of the force sensor including, but not limited to, via the package substrate **108**, which is arranged below the force sensor. Such application of force can produce a localized strain in the sensors. Example MEMS force sensors using piezoresistive sensing elements are described in U.S. Pat. No. 9,487,388, issued Nov. 8, 2016 and entitled "Ruggedized MEMS Force Die;" U.S. Pat. No. 9,493,342, issued Nov. 15, 2016 and entitled "Wafer Level MEMS Force Dies;" U.S. Pat. No. 9,902,611, issued Feb. 27, 2018 and entitled "Miniaturized and ruggedized wafer level mems force sensors;" and U.S. Patent Application Publication No. 2016/0363490 to Campbell et al., filed Jun. 10, 2016 and entitled "Ruggedized wafer level mems force sensor with a tolerance trench," the disclosures of which are incorporated by reference in their entireties.

As shown in FIG. **1**, the force sensor **102** can also include metal layer(s) **106**. The metal layers **106** can be made of any suitable conductive material, including but not limited to, aluminum, copper, or gold, for example. The metal layers **106** can provide electrical connection between the force sensor **102** and the package substrate **108**. For example, the force sensor **102** can be electrically and mechanically coupled to the package substrate **108** through solder bumps **107** provided on the bottom surface of the force sensor **102**. The solder bumps **107** are connected to the force sensor **102** at the metal layers **106**, which provide the electrical connection to the force sensor **102** such that an electrical signal can be transferred from the force sensor **102** to the package substrate **108**. It should be understood that solder bumps **107** are provided in FIG. **1** only as an example mechanism for mechanically and electrically connecting the force sensor **102** to the package substrate **108**.

The force sensor **102** can also include a compensation layer **109** (also sometimes referred to herein as "TCO compensation layer"). The compensation layer **109** can be formed from materials including, but not limited to, polymer, polyimide, resin, polycarbonate, acrylonitrile butadiene styrene (ABS), silicon oxide, glass, or combinations thereof. As shown in FIG. **1**, the TCO compensation layer **109** can be arranged on the top surface **104**A of the sensor substrate **104**. This disclosure contemplates that the force "F" can be applied to the force sensor **102** via the TCO compensation layer **109**, e.g., the TCO compensation layer **109** can be disposed on the top surface of the force sensor. As described herein, the compensation layer **109** has a thermal coefficient of expansion (TCE) that is different than a TCE of the sensor substrate **104**. In some implementations, the TCE of the compensation layer **109** can be less than the TCE of the sensor substrate **104**. In other implementations, the TCE of the compensation layer **109** can be greater than the TCE of the sensor substrate **104**. This disclosure contemplates that the thickness, the stiffness, the TCE, and/or the combination of thickness, stiffness, and TCE of the compensation layer **109** can be selected to reduce TCO. Alternatively or additionally, this disclosure contemplates that the thickness, the stiffness, the TCE, and/or the combination of thickness, stiffness, and TCE of the compensation layer **109** can be selected to minimize TCO. Optionally, the above characteristics of the compensation layer **109** can be selected to make TCO zero. Optionally, the above characteristics of the compensation layer **109** can be selected to make TCO a minimum but non-zero value based on design limitations (e.g., commercial, engineering, etc.). In other words, it should be understood that it may not be desirable or possible to reduce TCO to zero for every force sensor design. The effect of compensation layer stiffness on TCO is described below with regard to FIG. **5**. The effect of compensation layer thickness on TCO is described below with regard to FIG. **6**. Alternatively, as described above, the force "F" can be applied to the package substrate **108**. In this implementation, the force "F" can be applied via a TCO compensation layer and the TCO compensation layer can be designed as described above.

FIG. **2** illustrates the force sensor **102** (e.g., a MEMS force sensor) mounted on a package substrate **108**. The package substrate **108** can be a printed circuit board (PCB), a flexible printed circuit board (FPC), or a co-fired ceramic. It should be understood that PCBs, FPCs, and co-fired ceramics are provided only as example package substrates. The combined force sensor and package substrate is shown by reference number **201** in FIG. **2**. The force sensor **102** can include a dielectric layer **103**, a sensor substrate **104**, and a piezoresistive sensing element **105**. The sensor substrate, which can also be referred to as a sensor die, can be made of a semiconductor material such as silicon or gallium arsenide, for example. As shown in FIG. **2**, the sensor substrate **104** has a top surface **104**A and a bottom surface **104**B, which is opposite to the top surface **104**A. The piezoresistive sensing element **105** is arranged on the bottom surface **104**B. Optionally, in some implementations, a plurality of piezoresistive sensing elements **105** can be arranged on the sensor substrate **104**. This disclosure contemplates that the piezoresistive sensing element(s) **105** can be diffused, deposited, or implanted on the bottom surface **104**B. The dielectric layer **103** can then be arranged (e.g., deposited) over the bottom surface **104**B to electrically isolate the piezoresistive sensing element(s) **105**. Piezoresistive sensing elements are described above with regard to FIG. **1** and are therefore not described in further detail below.

As shown in FIG. **2**, the force sensor **102** can include a piezoelectric sensor in addition to the piezoresistive sensing element(s) **105**. This disclosure contemplates that the force sensor **102** can include a plurality of piezoelectric sensors. A piezoelectric sensor can include a piezoelectric sensing element **210** arranged between opposing electrodes. In FIG. **2**, the piezoelectric sensing element **210** is sandwiched between piezoelectric electrode **211** and metal layer **106** (e.g., the opposing electrodes). Piezoresistive and piezoelectric sensing elements can be used together in MEMS force sensors. For example, piezoresistive sensing elements are useful for sensing static forces applied to the force sensor **102**, while piezoelectric sensing elements are useful for sensing dynamic forces acting on the force sensor **102**. Thus, both piezoresistive and piezoelectric sensors can be used in conjunction to detect both static and dynamic forces. As described above, the piezoelectric sensing element **210** is located between piezoelectric electrode **211** and metal layer **106**. The piezoelectric sensing elements **105** can be configured to convert a change in strain to an analog electrical signal that is proportional to the change strain on the bottom surface **104**B. The piezoelectric sensing elements **210** sense dynamic forces applied to the force sensor **102**. Additionally, the electrical signals detected by the piezoresistive and piezoelectric sensing elements can be routed to digital circuitry. For example, the digital circuitry can be configured to, among other functions, convert the analog electrical signals to a digital electrical output signal. The use of both piezoresistive and piezoelectric sensing elements in a MEMS force sensor is described in detail in WO2018/148510, published Aug. 16, 2018 and entitled "INTEGRATED PIEZORESISTIVE AND PIEZOELECTRIC FUSION FORCE SENSOR," the disclosure of which is expressly incorporated herein by reference in its entirety.

As shown in FIG. **2**, the force sensor **102** can also include metal layer(s) **106**. The metal layers **106** can be made of any suitable conductive material, including but not limited to, aluminum, copper, or gold, for example. The metal layers **106** can provide electrical connection between the force sensor **102** and the package substrate **108**. For example, the force sensor **102** can be electrically and mechanically coupled to the package substrate **108** through solder bumps **107** provided on the bottom surface of the force sensor **102**. The solder bumps **107** are connected to the force sensor **102** at the metal layer **106**, which provides the electrical connection to the force sensor **102** such that an electrical signals can be transferred from the force sensor **102** to the package substrate **108**. It should be understood that solder bumps **107** are provided in FIG. **2** only as an example mechanism for mechanically and electrically connecting the force sensor **102** to the package substrate **108**.

The force sensor **102** can also include a compensation layer **109** (also sometimes referred to herein as "TCO compensation layer"). The compensation layer **109** can be formed from materials including, but not limited to, polymer, polyimide, resin, polycarbonate, acrylonitrile butadiene styrene (ABS), silicon oxide, glass, or combinations thereof. As shown in FIG. **2**, the TCO compensation layer **109** can be arranged on the top surface **104**A of the sensor substrate **104**. This disclosure contemplates that the force "F" can be applied to the force sensor **102** via the TCO compensation layer **109**, e.g., the TCO compensation layer **109** can be disposed on the top surface of the force sensor. As described herein, the compensation layer **109** has a thermal coefficient of expansion (TCE) that is different than a TCE of the sensor substrate **104**. In some implementations, the TCE of the compensation layer **109** can be less than the TCE of the sensor substrate **104**. In other implementations, the TCE of the compensation layer **109** can be greater than the TCE of the sensor substrate **104**. This disclosure contemplates that the thickness, the stiffness, the TCE, and/or the combination of thickness, stiffness, and TCE of the compensation layer **109** can be selected to reduce TCO. Alternatively or additionally, this disclosure contemplates that the thickness, the stiffness, the TCE, and/or the combination of thickness, stiffness, and TCE of the compensation layer **109** can be selected to minimize TCO. Optionally, the above characteristics of the compensation layer **109** can be selected to make TCO zero. Optionally, the above characteristics of the compensation layer **109** can be selected to make TCO a minimum but non-zero value based on the design limitations (e.g., commercial, engineering, etc.). In other words, it should be understood that it may not be desirable or possible to reduce TCO to zero for every force sensor design. The effect of compensation layer thickness on TCO is described below with regard to FIG. **6**. The effect of compensation layer stiffness on TCO is described below with regard to FIG. **5**. Alternatively, as described above, the force "F" can be applied to the package substrate **108**. In this implementation, the force "F" can be applied via a TCO compensation layer and the TCO compensation layer can be designed as described above.

FIG. **3** illustrates another force sensor **302** (e.g., a M EMS force sensor) mounted on a package substrate **310**. The package substrate **310** can be a printed circuit board (PCB), a flexible printed circuit board (FPC), or a co-fired ceramic. It should be understood that PCBs, FPCs, and co-fired ceramics are provided only as example package substrates. The combined force sensor and package substrate is shown by reference number **301** in FIG. **3**. The force sensor **302** can include a dielectric layer **303**, a sensor substrate **304**, a bond oxide layer **307**, a cap substrate **308**, and a piezoresistive sensing element **305**. The sensor substrate, which can also be referred to as a sensor die, can be made of a semiconductor material such as silicon or gallium arsenide, for example. As shown in FIG. **3**, the sensor substrate **304** has a top surface **304**A and a bottom surface **30413**, which is opposite to the top surface **304**A. The piezoresistive sensing element **305** is arranged on the bottom surface **30413**. Optionally, in some implementations, a plurality of piezoresistive sensing elements **305** can be arranged on the sensor substrate **304**. This disclosure contemplates that the piezoresistive sensing element(s) **305** can be diffused, deposited, or implanted on the bottom surface **30413**. The dielectric layer **303** can then be arranged (e.g., deposited) over the bottom surface **30413** to electrically isolate the piezoresistive sensing element(s) **305**. Piezoresistive sensing elements are described above with regard to FIG. **1** and are therefore not described in further detail below.

As described above, the force sensor **302** can include the sensor substrate **304** and the cap substrate **308**. The sensor substrate **304** and the cap substrate **308** can be bonded together via the bonded oxide layer **307**. It should be understood that the bonded oxide layer **307** is only provided as an example mechanism for bonding the sensor substrate **304** and the cap substrate **308**. For example, this disclosure contemplates bonding the substrates using other techniques known in the art including, but not limited to, silicon fusion bonding, anodic bonding, glass frit, thermo-compression, and eutectic bonding. The cap substrate **308** can optionally be made of glass (e.g., borosilicate glass) or semiconductor (e.g., silicon). The internal surfaces between the sensor substrate **304** and the cap substrate **308** form a sealed cavity **350**. The sealed cavity **350** can be formed by etching a trench from the sensor substrate **304** and then sealing a volume between the bonded sensor substrate **304** and cap substrate **308**. For example, the volume is sealed between the sensor substrate **304** and the cap substrate **308** when adhered together, which results in formation of the sealed cavity **350**. Example MEMS force sensors having a sealed cavity are described in U.S. Pat. No. 9,902,611, issued Feb. 27, 2018 and entitled "Miniaturized and ruggedized wafer level mems force sensors;" and U.S. Patent Application Publication No. 2016/0363490 to Campbell et al., filed Jun. 10, 2016 and entitled "Ruggedized wafer level mems force sensor with a tolerance trench," the disclosures of which are incorporated by reference in their entireties. The force sensor **302** therefore has a sealed cavity **350** that defines a volume entirely enclosed by the sensor substrate **304** and the cap substrate **308**. The sealed cavity **350** can be sealed from the external environment.

As shown in FIG. **3**, the force sensor **302** can also include metal layer(s) **306**. The metal layers **306** can be made of any suitable conductive material, including but not limited to, aluminum, copper, or gold, for example. The metal layers **306** can provide electrical connection between the force sensor **302** and the package substrate **310**. For example, the force sensor **302** can be electrically and mechanically coupled to the package substrate **310** through solder bumps **309** provided on the bottom surface of the force sensor **302**. The solder bumps **309** are connected to the force sensor **302** at the metal layer **306**, which provides the electrical connection to the force sensor **302** such that an electrical signal can be transferred from the force sensor **302** to the package substrate **310**. It should be understood that solder bumps **309** are provided in FIG. **3** only as an example mechanism for mechanically and electrically connecting the force sensor **302** to the package substrate **310**.

The force sensor **302** can also include a compensation layer **311** (also sometimes referred to herein as "TCO compensation layer"). The compensation layer **311** can be formed from materials including, but not limited to, polymer, polyimide, resin, polycarbonate, acrylonitrile butadiene styrene (ABS), silicon oxide, glass, or combinations thereof. As shown in FIG. **3**, the TCO compensation layer **311** can be arranged on the top surface **304**A of the sensor substrate **304**. This disclosure contemplates that the force "F" can be applied to the force sensor **302** via the TCO compensation layer **311**, e.g., the TCO compensation layer **311** can be disposed on the top surface of the force sensor. As described herein, the compensation layer **311** has a thermal coefficient of expansion (TCE) that is different than a TCE of the sensor substrate **304**. In some implementations, the TCE of the compensation layer **311** can be less than the TCE of the sensor substrate **304**. In other implementations, the TCE of the compensation layer **311** can be greater than the TCE of the sensor substrate **304**. This disclosure contemplates that the thickness, the stiffness, the TCE, and/or the combination of thickness, stiffness, and TCE of the compensation layer **311** can be selected to reduce TCO. Alternatively or additionally, this disclosure contemplates that the thickness, the stiffness, the TCE, and/or the combination of thickness, stiffness, and TCE of the compensation layer **311** can be selected to minimize TCO. Optionally, the above characteristics of the compensation layer **311** can be selected to make TCO zero. Optionally, the above characteristics of the compensation layer **311** can be selected to make TCO a minimum but non-zero value based on the design limitations (e.g., commercial, engineering, etc.). In other words, it should be understood that it may not be desirable or possible to reduce TCO to zero for every force sensor design. The effect of compensation layer thickness on TCO is described below with regard to FIG. **6**. The effect of compensation layer stiffness on TCO is described below with regard to FIG. **5**. Alternatively, as described above, the force "F" can be applied to the package substrate **310**. In this implementation, the force "F" can be applied via a TCO compensation layer and the TCO compensation layer can be designed as described above.

Referring now to FIG. **4**, deformation of an example MEMS force sensor due to an increase in temperature is shown. Such deformation has been exaggerated by 5000 times to provide clear visual examination. In FIG. **4**, a force sensor **401** is mounted to a package substrate **403** through solder bumps **402**. It should be understood that the force sensor **401** can be similar to one of the force sensors shown in FIG. **1-3** with the exception of including a compensation layer (e.g., compensation layer **109** or **311** in FIGS. **1-3**). In other words, the force sensor **401** can optionally include a sensor substrate, sensing element(s), a dielectric layer, and/or a cap substrate but does not include a TCO compensation layer. This disclosure contemplates that the bottom of the package substrate **404** is fixed for the purposes of the simulation, which mimics the actual operation conditions. In FIG. **4**, a temperature raise (e.g., an increase in temperature) is applied to the model for simulation from zero stress condition for TCO simulation. As shown in FIG. **4**, the package substrate **403** experiences thermal expansion as a result of the increase in temperature. Additionally, the deformation of the package substrate **403** is transferred to the force sensor **401** through the solder bumps **402**. The deformation shown in FIG. **4** causes negative TCO. Although deformation causing negative TCO is shown in FIG. **4**, this disclosure contemplates that deformation causing positive TCO can occur, for example, due to decreases in temperature.

Referring now to FIG. **5**, a graph illustrating normalized TCO versus normalized Young's modulus for an example compensation layer is shown. In FIG. **5**, TCO is normalized to the specific material and dimensions of an example MEMS force sensor. FIG. **5** illustrates the effect of varying the Young's modulus on TCO of the compensation layer. In the examples described herein, Young's modulus is provided as an example measure of the stiffness of the compensation layer material. Young's modulus is a known property that defines the relationship between stress and strain of a material. This disclosure contemplates that other measures of stiffness can be used. In some implementations, the TCE of the compensation layer is selected to be within the same order of magnitude of the TCE of the package substrate. In some implementations, the TCE of the compensation layer is selected to be about equal to the TCE of the package substrate. Optionally, the respective TCE of both the compensation layer and the package substrate can be larger than the TCE of silicon. As shown in FIG. **5**, by increasing the Young's modulus of the compensation layer, the TCO increases linearly and proportionally to the Young's modulus of the compensation layer. Additionally, at a particular Young's modulus, the TCO crosses over from negative to positive value. In FIG. **5**, this occurs where the normalized Young's modulus is about 2.0. Accordingly, by setting the Young's modulus appropriately, e.g., between about 1.5 to 2 for the example shown in FIG. **5**, the TCO can be tuned to zero.

In some cases, neither the Young's modulus nor the TCE of the compensation layer can be chosen without limitation. This is because both the Young's modulus and TCE are material properties, and there may be limitations (e.g., commercial, engineering, etc.) on the materials used. As described below, the thickness of the compensation layer affects the TCO. Referring now to FIG. **6**, a graph illustrating normalized TCO versus thickness of an example compensation layer is shown. In the example of FIG. **6**, the Young's modulus and TCE are set based on the material of the compensation layer. FIG. **6** illustrates the relationship between the TCO and thickness of the compensation layer. At some value, the TCO crosses from negative to positive value. In FIG. **6**, the TCO crosses over from negative to positive value around the normalized value of 1.9. Accordingly, by selecting a thickness of the compensation layer, the TCO can be reduced to zero at that specific thickness.

Although the subject matter has been described in language specific to structural features and/or methodological acts, it is to be understood that the subject matter defined in the appended claims is not necessarily limited to the specific features or acts described above. Rather, the specific features and acts described above are disclosed as example forms of implementing the claims.

What is claimed:

1. A microelectromechanical ("MEMS") force sensor for providing temperature coefficient of offset (TCO) compensation, the MEMS force sensor comprising:

a sensor substrate configured to receive an applied force, wherein the sensor substrate comprises a top surface and a bottom surface opposite thereto;

a sensing element arranged on the bottom surface of the sensor substrate, wherein the sensing element is configured to convert a strain on the bottom surface of the sensor substrate to an electrical signal that is proportional to the strain; and

a compensation layer arranged on the top surface of the sensor substrate, wherein the compensation layer has a thermal coefficient of expansion that is different than a thermal coefficient of expansion of the sensor substrate.

2. The MEMS force sensor of claim **1**, wherein the thermal coefficient of expansion of the compensation layer is less than the thermal coefficient of expansion of the sensor substrate.

3. The MEMS force sensor of claim **1**, wherein the thermal coefficient of expansion of the compensation layer is greater than the thermal coefficient of expansion of the sensor substrate.

4. The MEMS force sensor of claim **1**, wherein the thermal coefficient of expansion of the compensation layer is within the same order of magnitude of a thermal coefficient of expansion of a package substrate.

5. The MEMS force sensor of claim 1, wherein a thickness of the compensation layer minimizes TCO.

6. The MEMS force sensor of claim 5, wherein TCO is minimized at a value of about zero.

7. The MEMS force sensor of claim 1, wherein a stiffness of the compensation layer minimizes TCO.

8. The MEMS force sensor of claim 1, wherein the thermal coefficient of expansion of the compensation layer minimizes TCO.

9. The MEMS force sensor of claim 1, wherein a combination of a thickness, a stiffness, and the thermal coefficient of expansion of the compensation layer of the compensation layer minimizes TCO.

10. The MEMS force sensor of claim 1, wherein the MEMS force sensor is configured to for use as strain gauge.

11. The MEMS force sensor of claim 1, wherein the sensing element is a piezoresistive sensing element.

12. The MEMS force sensor of claim 1, wherein the sensing element is piezoresistive and piezoelectric elements.

13. The MEMS force sensor of claim 1, further comprising a cap substrate, wherein the sensor substrate and the cap substrate are bonded together forming a sealed cavity there between.

14. The MEMS force sensor of claim 1, wherein the MEMS force sensor is configured for electrical and mechanical coupling to a package substrate.

15. The MEMS force sensor of claim 14, wherein the MEMS force sensor is electrically and mechanically coupled to the package substrate, and wherein the package substrate is a printed circuit board (PCB).

16. The MEMS force sensor of claim 14, wherein the MEMS force sensor is electrically and mechanically coupled to the package substrate, and wherein the package substrate is a flexible printed circuit board (FPC).

17. The MEMS force sensor of claim 14, wherein the MEMS force sensor is electrically and mechanically coupled to the package substrate, and wherein the package substrate is a co-fired ceramic.

18. The MEMS force sensor of claim 1, wherein the compensation layer is formed of at least one of polymer, polyimide, resin, polycarbonate, acrylonitrile butadiene styrene (ABS), silicon oxide, glass, or combinations thereof.

19. The MEMS force sensor of claim 1, further comprising a plurality of sensing elements arranged on the bottom surface of the sensor substrate.

* * * * *